JKAU: Eng. Sci., **vol. 9**, pp. 125-139 (1417 A.H./1997 A.D.)

Effective Moment of Inertia of Partially Cracked RC Beams

RAJEH ZAID AL-ZAID
Civil Engineering Department, College of Engineering,
King Saud University, Riyadh, Saudi Arabia

ABSTRACT. Effective moment of inertia of an RC beam is shown to be function of the service load-level. The beam is subjected to, the reinforcement ratio in the beam and the type of loading (uniform or point loads). The well known formulas available for evaluation of effective moment of inertia considered the effect of uniformly distributed load only. The test results show that the effective moment of inertia under point loads is significantly different from that obtained from the formulas. Refined models are presented here, which account for the effects of all the loading types and are compared with the test results and with other models available for this purpose. Applicability of the models as well as other models to beams of T-sections is also investigated.

1. Introduction

The limiting of flexural deflection is one of the major serviceability design requirements in reinforced concrete beams. The design of structural members employing high strength materials yields rather slender members which are stressed to higher levels. This situation calls for more refined models than the ones available to predict their deflections.

The use of effective moment of inertia is widely accepted for computation of deflections of partially cracked RC beams under service loads. Branson[1,2] uses an interpolated value of the moment of inertia (MI), called effective moment of inertia, I_e, between the well defined limits of the uncracked and fully cracked states. The procedure employs loading level in the form of moment ratio, R_M, of the cracking moment, M_{cr}, to the applied service moment, M_a, for interpolation purposes. However, recent studies[3,4] show that I_e, besides R_M, depends upon the type of loading and the reinforcement ratio. The type of loading governs the extent of cracking along the reinforced concrete member, thereby in effect, rendering the beam 'nonprismatic'. A beam under a central point load tends to crack over a shorter length than the one under uniformly distributed load when subjected to the same R_M. On the other hand, the reinforcement ratio controls the rate at which cracks propagate towards the neutral axis, being slower for beams with higher steel percentages. IS-code[5] formula for I_e (which is based on the works by Beeby[6] and Brakel[7]) indirectly employs in addition to R_M, the effect of reinforcement in evaluation of I_e.

2. A Review and Discussion of the Available Formulae

There are several formulas which express I_e as function of the relevant parameters. The ACI code[2] adopted the well known Branson equation for I_e, which is

$$I_e = I_{cr} + [I_g - I_{cr}] (R_M)^m \leq I_g \tag{1}$$

where, $m = 3$, and I_g and I_{cr} are the moments of inertia of the gross and transformed cracked sections of RC beams, respectively. Among the relevant parameters affecting the value of I_e, Eq. (1) considers only the loading level which is reflected by the moment ratio, R_M.

In a recent study[3], two different approaches were used to incorporate the effect of the loading type in computation of I_e of normally reinforced beams. The first approach employed the format of Eq. (1) with different values of the exponent, m, for each load-type. The proposed values were 2.8, 2.3 and 1.8 for beams subjected to uniform, third-point, and midspan loads, respectively. The second approach incorporated the cracked length ratio, R_L, of the beam segment, L_{cr}, over which working moment exceeds M_{cr} to the beam span, L, besides the moment ratio to account for the type and level of the loading. The effective moment of inertia, I_e, is expressed in terms of R_L as,

$$I_e = I_g - (I_g - I_{cr}) (R_L)^{m'} \tag{2}$$

The exponent m' was found to be equal to R_M.

In a subsequent study[4], the effect on I_e of the reinforcement ratio, ρ, was also investigated. The study suggested modified values of the exponents m and m', to account for this effect. These values may be obtained from

$$m = a - 80\ \rho \tag{1 - a}$$

$$m' = 80\ \rho\ R_M \tag{2 - a}$$

For beams subjected to midspan point loads, the coefficient, a, was found to be $= 3$.

Another format for computation of I_e is available in the Indian Standard Code[5] equation, which is valid for I_e in the range $I_{cr} < I_e < I_g$

$$I_e = \frac{I_{cr}}{1.2 - R_M \frac{Z}{d} \left(1 - \frac{x}{d} \right) \frac{b_w}{b}} \tag{3}$$

where, Z = lever arm, x = depth of the neutral axis, d = effective depth, b_w = breadth of web, and b = breadth of compression zone. For rectangular sections b_w/b is unity. Equation (3) accounts for the effect of the reinforcement ratio, rather indirectly, by incorporating the x/d ratio, which is function of ρ. Other oversimplified models for computation of I_e are also available in the literature[8,9].

In view of the above discussion, the present work is aimed at accomplishing the following objectives :

(1) Comparison of the I_e values predicted by various available models with the test results of beams subjected to midpoint, third-point, and uniform loads.

(2) Generalization of the widely used Eq. (1) to account for the effect of reinforcement ratio on I_e of RC beams subjected to various types of loading.

(3) Modification of Eq. (3), which considers the effects of loading level and reinforcement ratio, to account for the effect of loading type.

3. Summary and Analysis of Test Results

Details of the test beams and their material properties, instrumentation, and loading patterns were reported earlier[3,4,10]. A summary of relevant information is presented in Table 1. Typical plots of the load-deflection curves of the experimental beams in the range beyond cracking are shown in Fig. 1. Tables 2 and 3 present the experimental and computed vales of I_e of the test beams for various moment ratios, R_M, for beams carrying point loads at midspan and uniform loads, respectively.

TABLE 1 Details of test beams used in the analysis.

Beam	f_c MPa	b, mm	h, mm	d, mm	$\rho \times 10^{-2}$	M_{cr}, kN · m	Reference
B1-U, B2-U	38.2	200	200	155	1.3	5.2	[3, 10]
B3-C, B4-C	38.2	200	200	155	1.3	5.3	[3, 10]
B5-T, B6-T	38.2	200	200	155	1.3	4.5	[3, 10]
B5-C, B10-C	25.5	200	200	155	2.0	3.7	[10]
B11-T, B12-T	25.5	200	200	155	2.0	2.5	[10]
B13-C	31.4	200	200	15	0.8	4.9	[10]
B14-T	31.4	200	200	155	0.8	3.1	[10]
B-L-11	33.0	200	240	188	0.8	5.1	[4]

1) U, C, and T in beam designations indicate uniform, midpoint and third-point loads, respectively.
2) Beam B-L-11 was tested under midpoint load.

Figure 2 shows the variation of the effective moment ratio, $R_I = I_e/I_{cr}$, with the moment ratio, R_M, determined from test results and predicted by Eq. (3). It can be seen that Eq. (3) does not distinguish between the differently loaded beams, while the experimental results show a noticeable difference. The plot of cracked length

TABLE 2. Comparison of computed and experimental values of effective moment of inertia for beam B-L-11[4].

R_M	R_L	$I_{exp} \times 10^6$ mm^4	I_e / I_{exp}				
			ACI Code	IS Code	Eq. (1)	Eq. (2)	Eq. (5)
0.603	0.397	112.81	0.80	0.554	0.93	0.93	0.96
0.567	0.433	99.74	0.84	0.609	0.98	0.98	1.01
0.539	0.461	92.16	0.86	0.645	1.01	1.01	1.03
0.495	0.505	84.63	0.86	0.681	1.00	1.01	1.04
0.458	0.542	79.34	0.86	0.707	1.00	1.01	1.04
0.435	0.565	75.98	0.86	0.726	1.00	1.02	1.05
0.402	0.598	71.76	0.87	0.752	1.00	1.02	1.06
0.360	0.640	67.75	0.87	0.774	0.99	1.01	1.06
0.318	0.682	64.03	0.88	0.797	0.98	1.00	1.05
0.294	0.706	60.37	0.92	0.833	1.01	1.03	1.08

Note: Details of test beam B-L-11 are:
b = 200 mm, h = 240, A_s = 308 mm^2 (2 ϕ 14), d = 188 mm, ρ = 0.8%,
I_{cr} = 50.86 × 10^6 mm^4, I_g = 230.4 × 10^6 mm^4, $Z(1 - x/d)/d$ = 0.642.
Type of load: Point load at midspan.

TABLE 3. Comparison of computed and experimental values of effective moment of inertia for beams B1-U and B2-U[3,10].

R_M	R_I	$I_{exp} \times 10^6$ mm^4	I_e / I_{exp}				
			ACI code	IS code	Eq. (1)	Eq. (2)	Eq. (5)
0.735	0.51	73.45	1.03	0.67	1.07	1.04	0.98
0.676	0.57	67.34	1.00	0.70	1.04	1.03	0.98
0.625	0.61	62.85	0.97	0.72	1.02	1.02	0.98
0.578	0.65	58.98	0.96	0.75	1.00	1.01	0.98
0.505	0.70	54.34	0.93	0.77	0.97	1.00	0.97
0.450	0.74	50.35	0.93	0.81	0.96	1.00	0.98
0.405	0.77	47.54	0.93	0.83	0.96	1.01	0.99
0.368	0.79	45.87	0.93	0.84	0.96	1.01	0.99
0.338	0.81	44.57	0.94	0.85	0.96	1.01	0.99
0.312	0.83	43.62	0.94	0.86	0.96	1.00	0.98
0.289	0.84	42.83	0.94	0.86	0.96	1.00	0.98

Note: Details of test beams B1-U and B2-U are:
b = 200 mm, h = 200 mm, A_s = 402 mm^2 (2 ϕ 16), d = 155 mm, ρ = 1.3%,
I_{cr} = 38 × 10^6 mm^4, I_g = 133.33 × 10^6 mm^4, $Z(1 - x/d)/d$ = 0.585.
Type of load: Uniform load.

ratio, R_L, as determined from the fundamentals of structural analysis, versus moment ratio, R_M, produced in Fig. 3 clearly suggests that the difference is due to the variation in the extent of cracked length under the different loading types. The figure reveals that, at the same moment ratio, R_M, the three differently loaded beams have different cracked lengths which definitely affect the averaging concept employed in the computations of I_e.

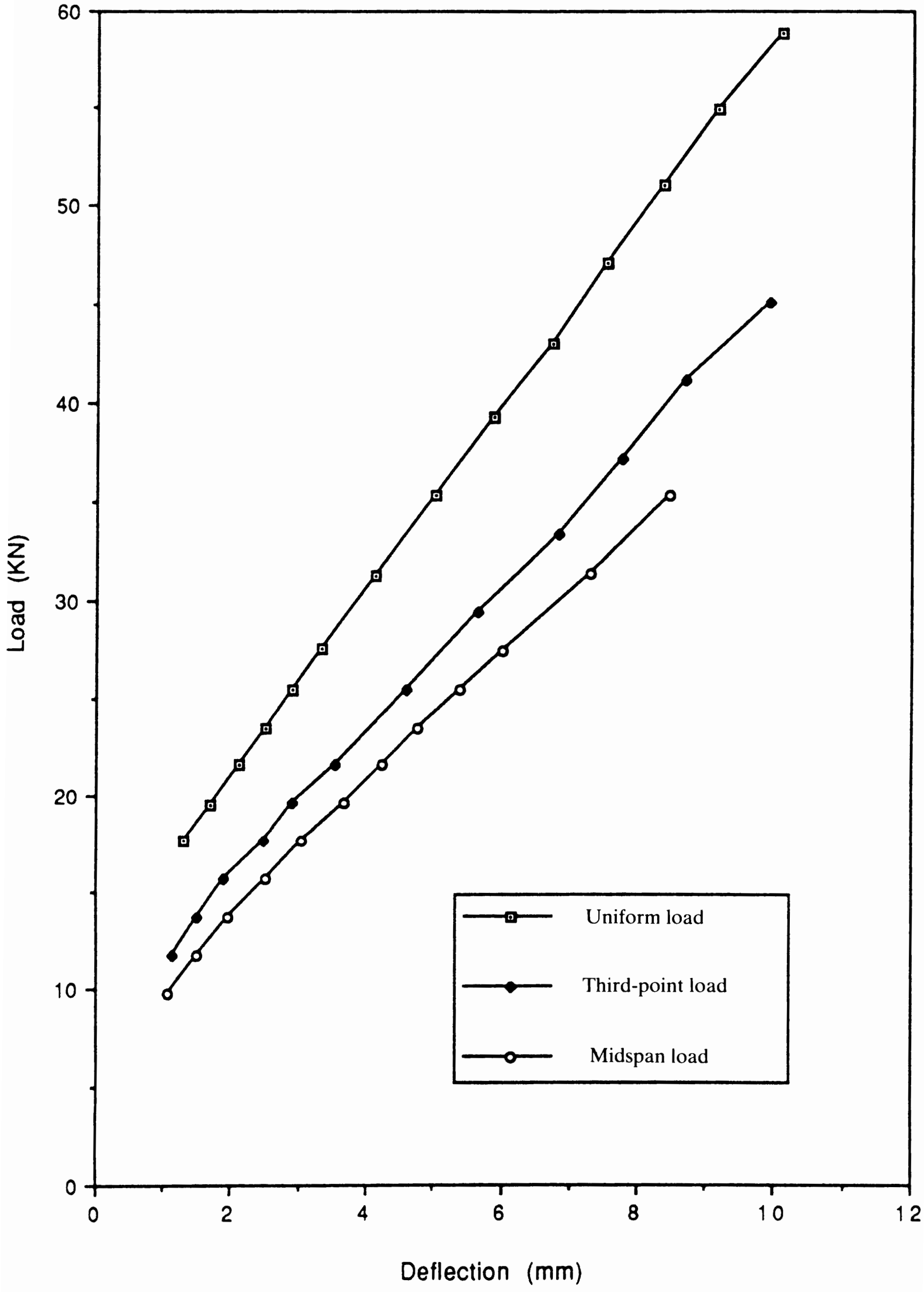

FIG. 1. Typical load-deflection curves of the experimental beams[3,4].

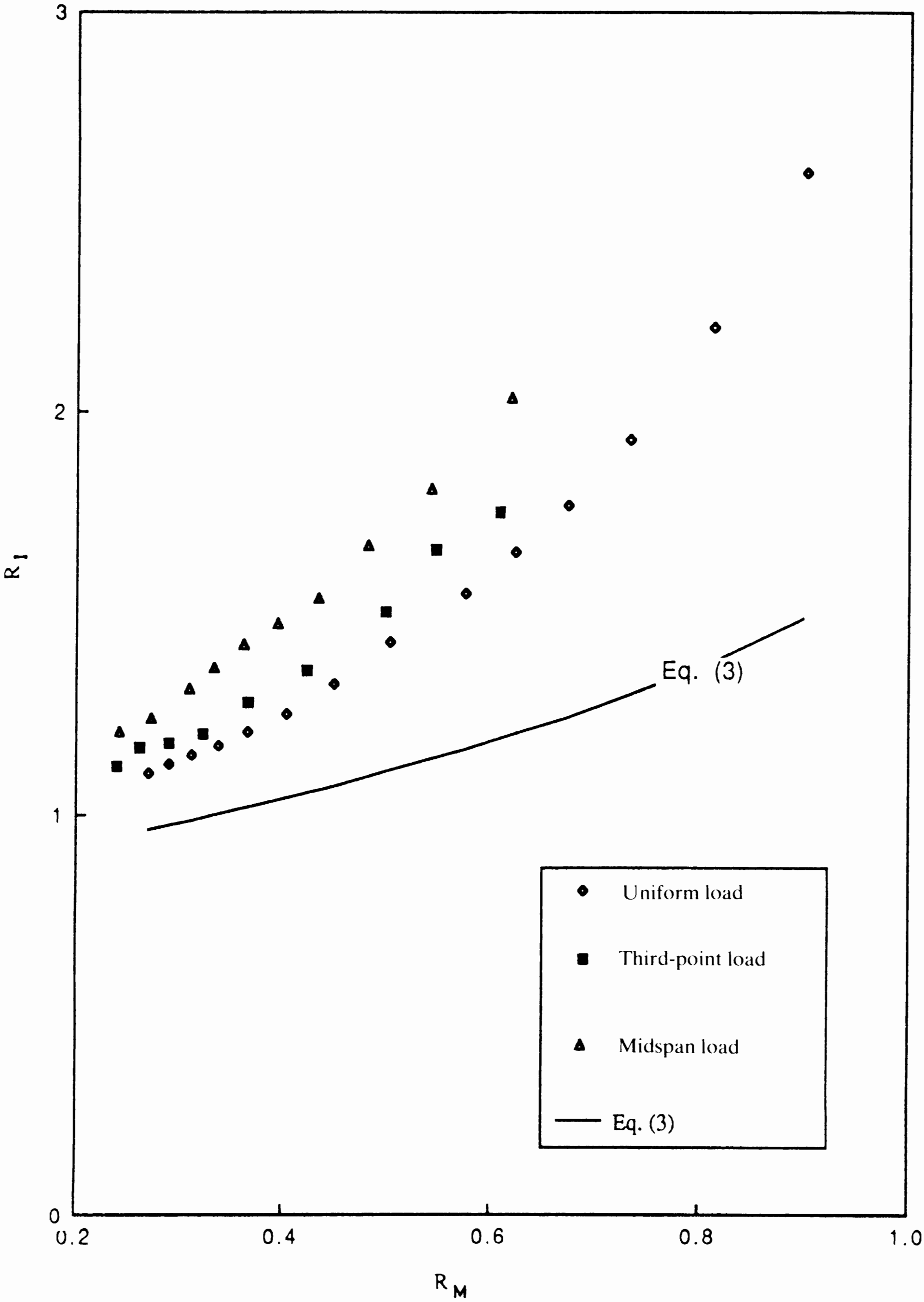

FIG. 2. Variation of R_I with R_M.

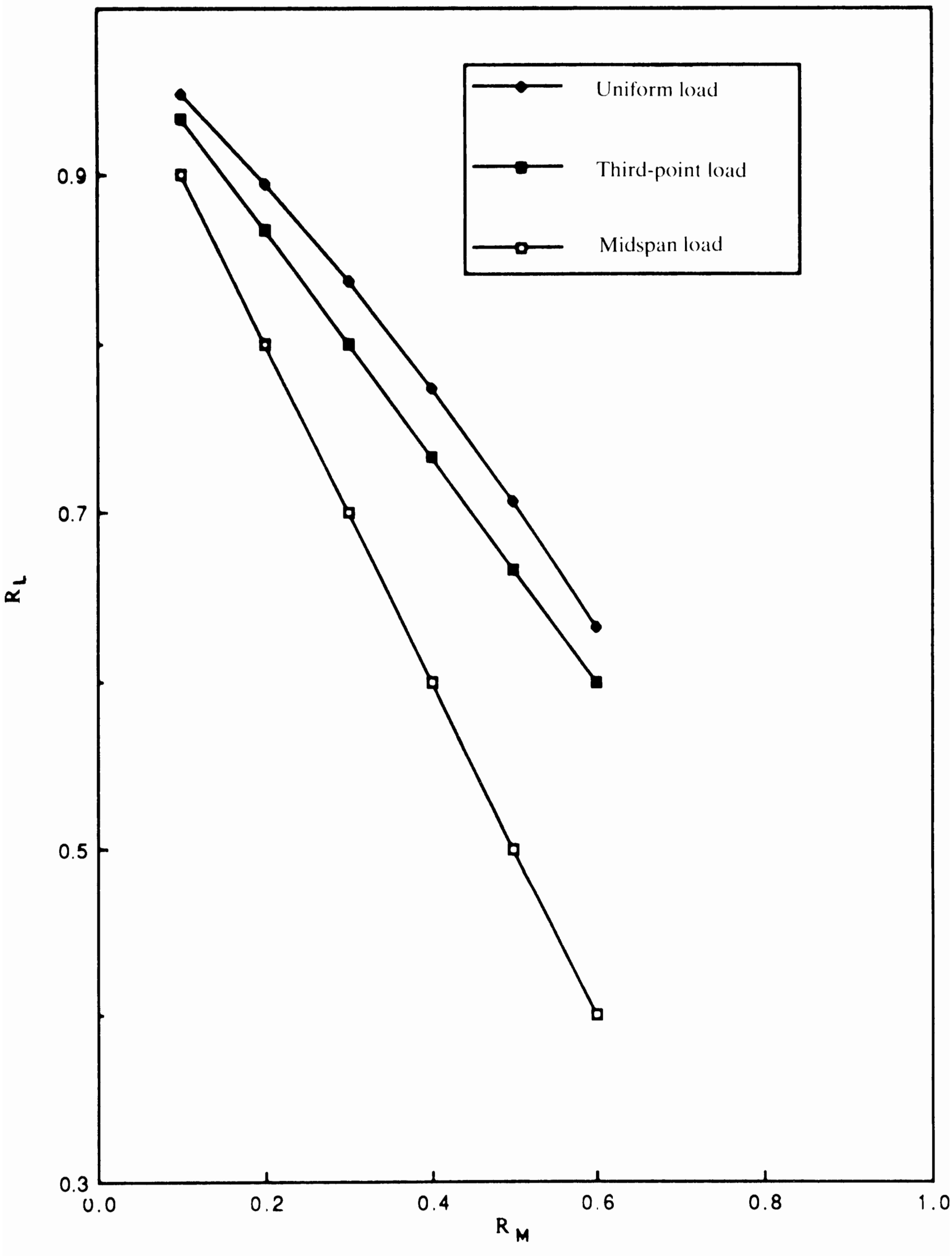

FIG. 3. Theoretical values of R_L vs. R_M.

Figure 4 compares the experimental values of R_I with the computed ones using Eq. (3). The figure suggests that Eq. (3) needs to be modified to account for the effect of type of loading and to overcome the inconsistency in the prediction error, which is higher for lightly cracked beams.

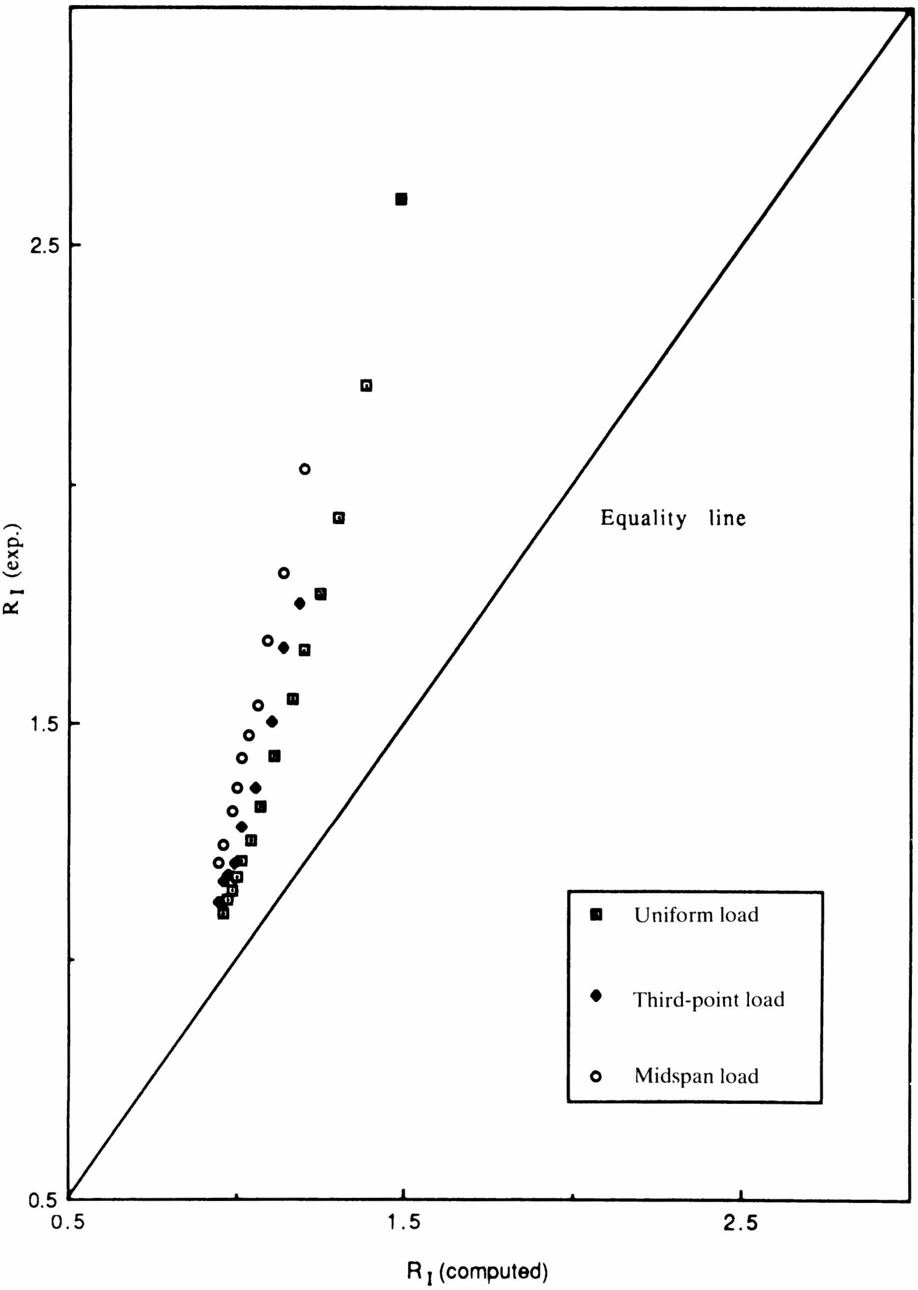

FIG. 4. Experimental values of R_I vs. the corresponding theoretical values computed by using Eq. (3).

4. Proposed Models

Equation (1) is modified to account for the effect of the reinforcement ratio on the I_e values for RC beams under a general state of loading. The test results, which were reported earlier[3,4,10] on the beams summarized in Table 1, are utilized. The case of beams under central point loads was investigated in Ref. [4]. A relation in the form of Eq. (1-a) is obtained by linear fitting for beams under third-points loads, and by extrapolation for beams under uniform load. The extrapolation is based on the reported value of m at $\rho = 1.3\%$ from Ref. [3]. The values of the coefficient, a, to be used in Eq. (1-a) are summarized in Table 4.

TABLE 4. Coefficients a, α and β for the various load types.

Loading type	a	α	β
Uniform load	3.8	1.15	- 1.45
Third-point load	3.5	1.10	- 1.50
Midpoint load	3.0	1.07	- 1.55

In order to incorporate the effect of type of loading in Eq. (3) while maintaining its form, the ratio of effective MI, R_I, is modeled as :

$$R_I = \frac{1}{\alpha + \beta X_M} \tag{4}$$

where, $X_M = R_M (Z/d)(1 - X/d)\, b_w/b$, & α & β are coefficients to be determined by regression analysis of the experimental test data.

The experimental values of R_I^{-1} for the differently loaded rectangular beams summarized in Table 1, are then plotted against the corresponding X_M values as shown in Fig. 5. The linear regression coefficients α and β for the three loading types are presented in Table 4. Thus, I_e may be expressed as

$$I_e = \frac{I_{cr}}{\alpha + \beta R_M \frac{z}{d}\left(1 - \frac{x}{d}\right)\frac{b_w}{b}} \tag{5}$$

Computed values of ratio of effective MI, R_I, from Eq. (5), at various moment ratios, are compared with the corresponding experimental values of R_I[3,4] in Fig. 6. The plot shows that Eq. (5) adequately accounts for the effect of loading type in the computation of I_e.

5. Comparison of the Various Models

Accuracy of the effective MI models presented in this work is checked against typical test results from Ref. [3,4 and 10] on beams with rectangular and T-sections. The effect on I_e of the parameters like the level and the type of loading, and the reinforcement ratio is compared.

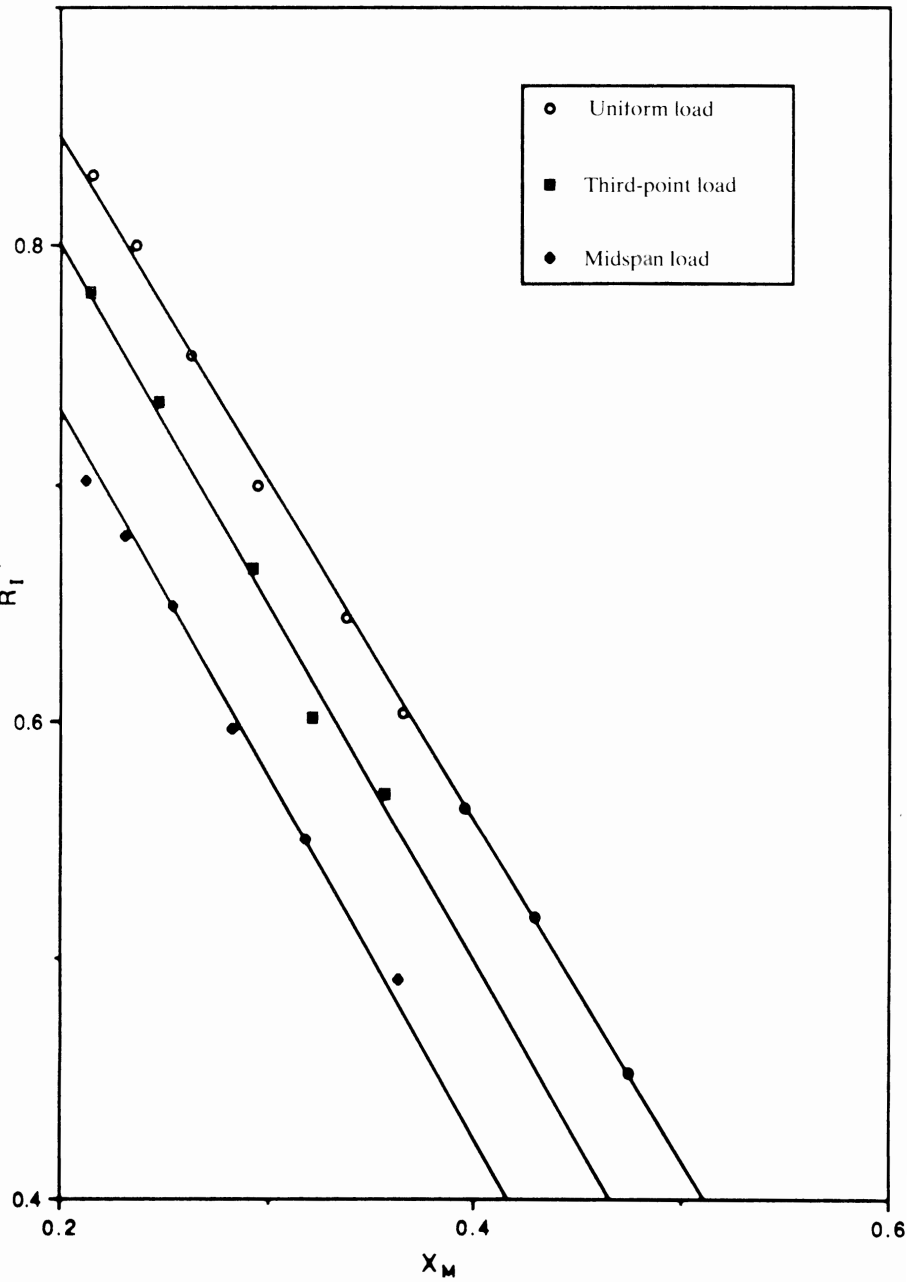

FIG.5 Variation of R_I^{-1} with X_M for different types of load.

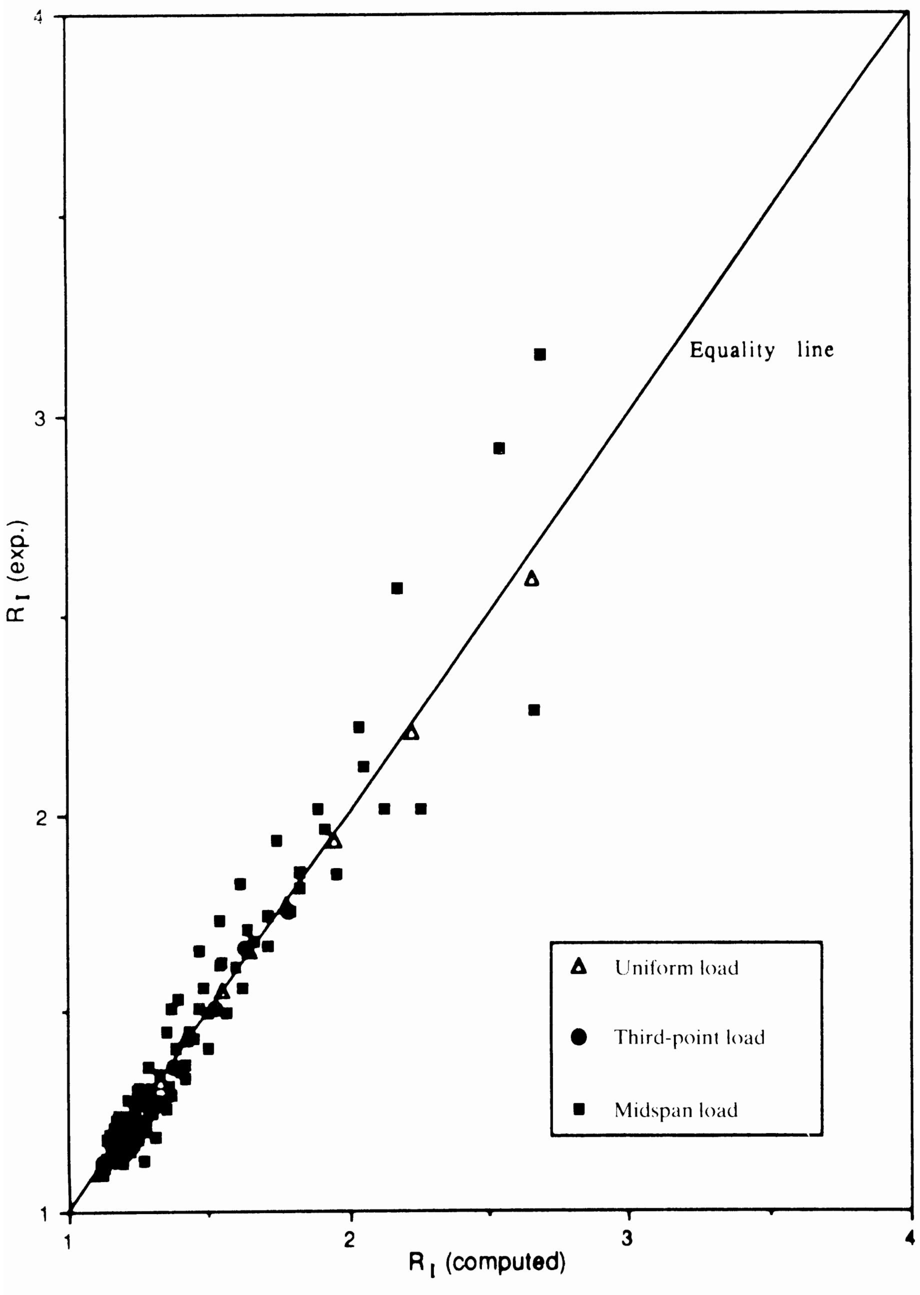

FIG. 6. Experimental values of R_I vs. the corresponding theoretical values by using Eq. (5).

5.1 Rectangular Sections

Table 2 presents the experimental values of a loaded rectangular beam under a central point load[4] and compares them with values obtained from ACI-Code formula, IS-Code formula, Eq. (1), Eq. (2) and the proposed Eq. (5), which is a modified version of the IS-Code formula. Table 3 does the same for the average values obtained for two identical uniformly loaded beams[3]. The following observations are made on the information presented in these tables :

1. The IS-Code formula, Eq. (3), underestimates I_e of both the centrally and the uniformly loaded beams.
2. As mentioned previously, the ACI-Code formula was derived on the basis of experimental results of uniformly loaded beams. This explains the good agreement with the test results in Table 3.
3. Equations (1) and (2) show a superior ability to predict I_e under all circumstances. Equation (5) is also fairly accurate as compared to its original version in the form of Eq. (3).

5.2 T-Sections

Table 5 reports the results of two T-beams carrying a midspan and third-point loads. Pertinent information of the test beams is summarized in the footnote of the table. The values of R_l using Eq. (1), (2), and (5) show good agreement with the test results. On the other hand, the IS-Code formula is observed to be the least accurate.

TABLE 5. Applicability of available and proposed models to beams of T-sections[10].

Beam designation	R_M	R_L	$I_{exp} \times 10^6$ mm^4	I_e / I_{exp}				
				ACI-code	IS-code	Eq. (1)	Eq. (2)	Eq. (5)
B15-3M midspan load	0.600	0.400	91.85	0.93	0.69	1.03	1.04	0.84
	0.429	0.571	75.60	0.94	0.83	1.03	1.04	0.94
	0.333	0.667	71.82	0.93	0.88	0.99	1.01	0.94
	0.273	0.727	67.54	0.96	0.93	1.01	1.02	0.98
	0.231	0.769	66.21	0.97	0.95	1.00	1.02	0.98
B16-3T third-point load	0.571	0.619	81.08	1.01	0.78	1.04	1.00	0.89
	0.444	0.704	77.62	0.93	0.81	1.95	0.95	0.88
	0.364	0.757	69.68	0.97	0.90	0.99	1.00	0.95
	0.308	0.795	67.41	0.98	0.93	0.99	0.99	0.96
	0.267	0.822	65.21	1.00	0.97	1.01	1.02	0.97

Note: Details of test beams B15-3M and B16-3T are:
b = 350 mm, b_w = 150 mm, h = 210 mm, h_f = 60 mm, d = 165 mm, A_s = 509 mm^2 (2 ϕ 18), ρ = 0.88%,
I_{cr} = 63 × 10^6 mm^4, I_g = 165 × 10^6 mm^4, $Z(1 - x/d)/d$ = 0.631.

6. Conclusion

The study points to the fact that effective moment of inertia of an RC beam depends upon the service load level, the reinforcement ratio and the load type applied to the beam. Various models, currently in use, only account for either the load level or the load level and reinforcement ratio. This study presents refined models which, in addition to the above mentioned factors, consider the load type. The models are compared with the test results.

The ρ-and-load-type-dependent value of exponent m given by Eq. (1-a) enables Eq. (1) to account for both the reinforcement ratio and the loading type with an excellent accuracy.

In case of rectangular beams carrying midspan load, the effective moment of inertia, I_e. by the IS-Code formula, at various moment ratios, varies from the experimental values by – 44.6% to – 16.7%, while I_e obtained by using the modified version of the formula does so by – 4% to + 8%. These variations in case of T-beams carrying midspan load range from – 31% to – 5% and from – 16% to – 2%, respectively. However, more test data is necessary to strengthen the above conclusions.

References

[1] **Branson, D.E.,** *Instantaneous and Time-Dependent Deflections of Simple and Continuous Reinforced Concrete Beams,* HPR Report No. 7, Part 1, Alabama Highway Department, Bureau of Public Roads, 1963, pp. 1-78 (1965).

[2] **ACI Committee 318,** *Building Code Requirements for Reinforced Concrete,* (ACI, 318-71), American Concrete Institute, Detroit, p. 78 (1971).

[3] **Al-Zaid, R.Z., Al-Shaikh, A.H.** and **Abu-Hussein, M.M.,** Effect of loading type on the effective moment of inertia of reinforced concrete beams, *ACI Structural Journal,* **88**(2): 184-190 (1991).

[4] **Al-Shaikh, A.H.** and **Al-Zaid, R.Z.,** Effect of reinforcement ratio on the effective moment of inertia of reinforced concrete beams, *ACI Structural Journal,* **90**(2): 144-149 (1993).

[5] **Bureau of Indian Standards,** *IS 456/1978, Indian Standard Code of Practice for Plain and Reinforced Concrete* (Third Revision), New Delhi, p. 148.

[6] **Beeby, A.W.,** *Short-Term Deflections of R.C. Members,* Cement and Concrete Association, Technical Report, TRA 408, London, p. 18 (1968).

[7] **Brakel, I.J.,** Calculation and limitation of deflection, CEB, *Bulletin of Information,* **90** (1977).

[8] **Grossman, J.S.,** Simplified computations for effective moment of inertia I_e and minimum thickness to avoid deflection computations, *ACI Journal,* **78**(6): 423-439 (1981).

[9] **Rangan, B.V.,** Control of beam deflections by allowable span-depth ratios, *ACI Journal,* **79**(5): 372-377 (1982).

[10] **Abu-Hussein, M.M.,** *Effective Moment of Inertia of Cracked Reinforced Concrete Beams Under Different Types of Loading,* M.Sc. Thesis, King Saud University, Civil Engineering Department, Riyadh, p. 116 (1989).

Notation

s	:	Numerical coefficient
A_s	:	Area of reinforcing steel
b	:	Breadth of compression zone
b_w	:	Breadth of web of a flanged section
d	:	Effective depth of beam section
f'_c	:	Compressive strength of concrete
h	:	Height of beam section
h_f	:	Depth of flange of a flanged section
I_{cr}	:	Moment of inertia of the transformed cracked section
I_e	:	Effective moment of inertia of the partially cracked beam
I_{exp}	:	Experimental value of I_e
I_g	:	Moment of inertia of the gross concrete section

L	:	Beam span
L_{cr}	:	Cracked length (beam segment over which the working moment exceeds M_{cr})
m	:	Exponent for use in Eq. (1)
m'	:	Exponent for use in Eq. (2)
M_a	:	Maximum service load moment acting on the beam
M_{cr}	:	Cracking moment of beam
R_I	:	Ratio of effective moment of inertia, I_e/I_{cr}
R_L	:	Ratio of cracked length, L_{cr}/L
R_M	:	Ratio of moment, M_{cr}/M_a
X	:	Depth of neutral axis
Z	:	Lever arm
ρ	:	Reinforcement ratio
α, β	:	Numerical coefficients.

عزم القصور الذاتي الفعال للعوارض الخرسانية المسلحة المتشققة جزئيًّا

راجع زيد الزيد

قسم الهندسة المدنية ، كلية الهندسة ،
جامعة الملك سعود ، الرياض ، المملكة العربية السعودية

المستخلص . أثبتت الدراسة اعتماد عزم القصور الذاتي الفعال للعوارض الخرسانية المسلحة على كل من مستوى حمل التشغيل ونسبة حديد التسليح ، وكذلك على نوع الحمل من حيث توزيعه أو تركيزه على العارضة . حيث أثبتت التجارب أن عزم القصور الذاتي الفعال للعوارض الخرسانية المسلحة المحملة بأحمال مركزة يختلف بدرجة كبيرة عنه بالنسبة للعوارض المحملة بأحمال موزعة ، والتي تم على أساسها تطوير النماذج الموجودة لحساب عزم القصور الذاتي الفعال . لذا فإن هذه الدراسة تقدم نماذج معدلة تأخذ في الاعتبار جميع أنواع الأحمال التي يمكن أن تتعرض لها العوارض الخرسانية ، كما تمت مقارنتها مع النتائج التجريبية ومع النماذج الأخرى الموجودة لهذا العرض . تم أيضا فحص إمكانية استخدام النماذج المقترحة بالنسبة للعوارض الخرسانية ذات مقطع على شكل حرف T .